Examining sliding in rotor assemblies: an experimental study

N. Abuhemeida [1,2], **D. Vaillant** [1], **G. Chevallier** [2], **F. Cronfalt** [1], **M. Topenot** [1], **M. Ouisse** [2]
[1] Alstom Transport,
7 Av. Mal de Lattre de Tassigny, 25290 Ornans, France

[2] SUPMICROTECH, Université de Franche-Comté, CNRS, Institut FEMTO-ST,
15B Av. des Montboucons, 25000 Besançon, France

Abstract
This study investigates the sliding phenomenon at the fan-hub interface within an electric traction motor, and its impact on the mechanical integrity of the fan for railway applications. Focusing on the most crucial vibration mode, a set of structured tests were conducted on an inertia-equivalent rotor in order to exclude any unwanted interference compared to a full-size rotor. The bolts which hold the fan-equivalent part in place were equipped with strain sensors for real time monitoring, while the collected time signals from the accelerometers allowed to compare the vibration behavior amongst different bolt tightening levels and different excitation levels.

1 Introduction

Rotor assemblies are key components in various mechanical systems, such as turbines and engines. Understanding how different parts of these assemblies interact with each other is crucial for their performance and durability, where the ill quantification of these details can pose serious concerns over the functionality of the machine as a whole. This study focuses on examining, quantifying, and studying the effect of the sliding phenomenon at the fan-hub interface of rotor assemblies as a part of an electric traction motor for railway application under its most crucial vibration mode.
When it comes to train industry, many researches have addressed the train drive system's mechanical integrity through the stability of its main components rather than focusing on the motor's sub-components, such as the bogie frame [1], the motor hangers [2], the gearbox housing [3][4], and the motor-suspending device connecting bolts [5]. On the other hand, many studies have addressed the effect of the bolts loosening in other mechanical structures.
In an attempt to detect bolts loosening in a truss, PZT patches were fixed on the joints to assess the relative deviation in the impedance curve for a mode dense frequency range. While one indicator could successfully detect the changes in the bolt tightening, the results are highly sensitive to the location of the patch and might not be able to detect tightening level variation in some cases [6].
In 2004, and as a part of a health monitoring system for high speed space vehicles, a study focusing on the bolt joints of the thermal protection system found that using a narrowband activation signal near the natural frequency was ineffective in distinguishing between healthy and loosen states. Widening the excitation band, the difference between the two extreme states, fully tightened and zero pressure applied, was demonstrated through FRF and summed spectral energy across the frequency band [7].
Another study in the same year have also used a modal approach to differentiate between two states of self-sensing and self-repairing bolted joints as a global indicator of the decreased tightening level [8].
In 2006, Jinkyu Yang and Fu-Kuo Chang proposed an attenuation-based method for detecting bolt loosening in C–C composite thermal protection panels, using a five-peak tone burst signal on one bolt of the joining bracket and measure the transient response on the other. by employing energy and specific damping capacity (SDC) as features, the team managed to assess the integrity of the studied bolts [9][10].

Other studies like [11][12] opted for ultrasonic measurement based on the acoustoelastic principle to be able to quantitatively measure stress levels for tightened bolts, but again this kind of studies focused on the joint integrity itself rather than its effect on the mechanical behavior of the structure as a whole.

In this work, the primary focus is not only on detecting sliding at the interface caused by bolt loosening, but also on investigating whether or not this phenomenon impacts the health integrity of the motor's fan in specific. Moreover, and in addition to the widely applied modal approach, a new approach was also tested analyzing the time signals induced by a single frequency excitation, focusing on the evolution of the amplitude and the phase shift for different tightening levels.

In order to validate the methodology and avoid the presence of numerous potential nonlinear effects, the experimental tests were conducted on a simplified prototype of equal inertia rather than a full-size rotor, targeting the mode that has the highest ability to effectuate sliding at the fan-hub interface, then analyzing the collected time response signals thanks to the 3D accelerometers mounted on each side of this interface. Additionally, the six bolts that connects the fan to the hub were equipped with strain sensors, which made it possible to control the tightening tension with high precision as well as to monitor bolt tension in real-time. Multiple sets of experiments were conducted systematically varying tightening level and excitation level.
This study contributes to the understanding of sliding phenomena in rotor assemblies, providing practical insights for the fan mechanical integrity in train motors, aiming to improve their performance and reliability in intended industrial applications.

2 Test preparation

As an important part of the train motor, understanding the behavior of the fan and its interaction with the connected parts is crucial to insure the credibility and possibly improve the efficiency of the train motor as a whole. A set of experimental tests were conducted initially on a full-size rotor equipped with two symmetrically attached arms to facilitate the application of the designated loading and to insure the excitation of the targeted vibration mode. Even though this stage provided insight into a case closer to the actual operation condition, but in this paper we will focus on the tests conducted on an inertia-equivalent prototype which helped to better isolate the studied phenomenon by mitigating the nonlinear effects and the setup uncertainties observed in the actual rotor. Figure 1 shows the full-size rotor setup and how its parts are represented in the equivalent prototype.

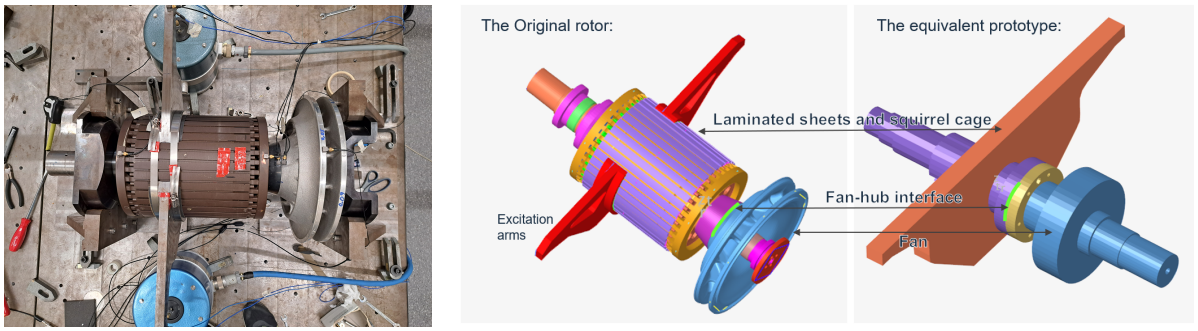

(a) Preliminary test bench - top view

(b) Rotor parts representation in the equivalent prototype.

Figure 1: preliminary test bench and the equivalence between the original rotor and the simplified prototype.

2.1 Experimental setup

As shown in Figure 2a, the equivalent rotor is fixed at both ends but can rotate freely around its longitudinal axis, where the structure can be excited through a shaker with a flexible stinger attached directly to the rotor's body.

(a) Test bench. (b) The studied interface.

Figure 2: The experimental test bench with a close-up of the instrumented bolts and the 3D accelerometers mounted on both sides of the studied interface.

In order to fully capture the mode shape, 3D accelerometers were mounted at the extremities of the shaft and the middle mass, in addition to two accelerometers on both sides of the interface were the fan is connected to the hub, which will be referred to in this study as the fan-hub interface or simply the studied interface. Moreover, the six bolts holding the fan in place were equipped with strain sensors, enabling precise control of the applied tension, as well as real-time monitoring of tension during vibration tests. Figure 2b.

2.2 Methodology

2.2.1 Data collection

Determination of the critical vibration mode frequency

Since the main goal is to induces sliding at the fan-hub interface, the vibration mode that has the highest potential should be specified with good precision, and then excited using a high force to obtain the desired effect. Bearing in mind the nonlinear nature of the tested structure, the FEM model will be able to provide the needed information only for a case with low excitation level and highest tightening level at the studied interface, while in any different scenario the mode location has to be found experimentally. To achieve this, the FEM model served solely as guidance for the expected mode shape and approximate frequency. From there, a structured set of tests was designed to observe the change in vibration response induced by reducing the tightening level at the studied interface. For each test, representing a new state of the structure, a random noise test was implemented to locate the mode, which was then verified through manual sine sweep excitation around the nominal value. Finally, the eigenvalue for the critical mode was determined as the one that induced the highest response amplitude within the tested range, with continuous verification of the mode shape to ensure consistency and avoid transitioning to a different vibration mode.

Implemented tests

the highest applied tightening level that corresponds to the experimental healthy joint is 15000 N applied on each of the six bolts at the studied interface. This tension force has been uniformly controlled and varied across all six bolts thanks to the strain sensor integrated into each one. The examined cases were as follows: 15000 N, 12000 N, 9000 N, 6000 N, 3000 N, 2000 N, and 1000 N.

For each tightening level, and after the determination of the critical mode frequency as detailed previously, the structure was stimulated at this frequency using two excitation levels: 1.4V, the highest possible before overloading the amplifier, and 0.1V, a relatively low level for comparison.
This set of 14 tests (7 tightening levels * 2 excitation levels) were implemented 4 times to insure the repeatability of the results.

Type of collected data

The team considered three types of collected signals to observe the loosening effect:

- The FRF at the excitation point where the shaker is attached, Figure 2a, to observe the evolution of the targeted mode frequency;
- The real time tension in the bolts, to detect any change during the vibration test itself;
- The time signals from the two accelerometers mounted on either side of the studied interface, to analyze the evolution of the amplitude ratio and the phase shift between for each tightening level and excitation level.

2.2.2 Post processing

In this paper, we introduce a signal processing methodology aimed at analyzing time signals to study differences at the fan-hub interface under various tightening levels. For this purpose two approaches were adopted:

Intra-side signal comparison using a fixed reference level

In this approach, global statistical methods were employed to get an overall understanding of the evolution of the time signal on each side independently compared to the reference state at 15000 N tightening level. Two indicators were used:

- The maximum cross-correlation: which can help detect the similarity between two signals as a function of the time-lag applied to one of them. Since the comparison is one sided, then the specific lag is meaningless, and the comparison will be done between the maximum cross-correlation values regardless of the lag.
- P-value of t-test: a statistical value used to compare the means of two groups, which directly reflects, in our case, the ability of detecting any shift in the oscillation center.

Inter-side signal comparison at same bolt tightening levels

This approach is crucial for quantifying the differences between each side of the studied interface in terms of the amplitude ratio and the phase shift, as well as how these differences evolve throughout the loosening process. For this purpose, the two following methods were tested:

- Nonlinear signal fitting (NLF) of the form: $A + B\cos(\omega t) + C\sin(\omega t)$.
- The Hilbert transformation.

Before evaluating each method, a simplified two Degrees of Freedom (2DoF) system was examined, serving as a theoretical reference for the behavior of a bolted joint subjected to loosening.

The system presented in Figure 3a shows 2DoFs where the first (m_1, k_1, c_1) is connected to the ground and subjected to an external force F, whereas the second (m_2, k_2) is not. The two DoFs are held together with a normal force N, and a dahl model (F_d, a, μ) is defined to represent the friction effect. The state vector $\mathbf{Q}$ and its derivative $\dot{\mathbf{Q}}$ for this system are:

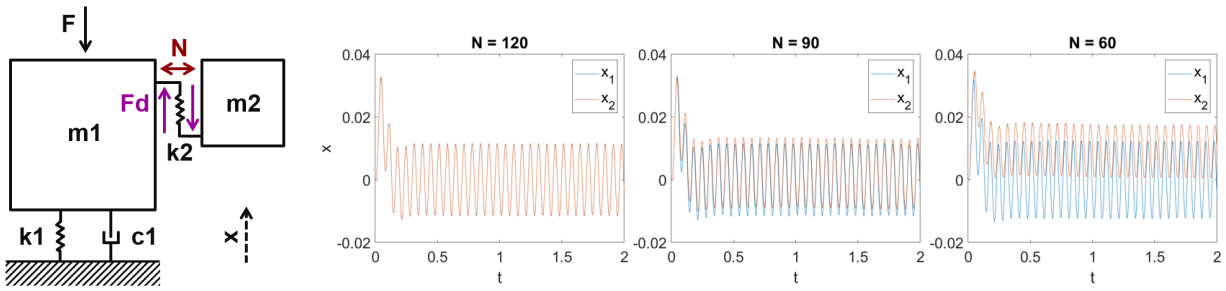

(a) The 2DoF system. (b) Loosening effect on the response of each DoF - parameter-dependent results.

Figure 3: Numerical testing of a simplified 2DoF system: Loosening effects on the amplitude and the phase for a specific set of parameters.

$$\mathbf{Q} = \begin{bmatrix} x_1 \\ x_2 \\ dx_1 \\ dx_2 \\ F_d \end{bmatrix}, \quad \dot{\mathbf{Q}} = \begin{bmatrix} dx_1 \\ dx_2 \\ \frac{1}{m_1}\left(-c_1 dx_1 - k_1 x_1 + F_d + F + k_2(x_2 - x_1)\right) \\ \frac{1}{m_2}\left(-F_d - k_2(x_2 - x_1)\right) \\ \sigma\left(1 - \frac{F_d}{N\mu}\text{sign}(dx_2 - dx_1)\right)^a (dx_2 - dx_1) \end{bmatrix}$$

As shown in Figure 3b, in a global loosening situation the amplitude ratio and the phase shift between the two connected DoFs are expected to change. It should be noted that the amplitude ratio might increase or decrease depending on the definition of each DoF. Therefore, it is necessary to test the sensitivity of NLF and Hilbert transformation accuracy regarding amplitude ratio, phase shift, and oscillation center shift. A set of well defined signals with one or multi peaks were generated for this purpose, where the user can force a specific amplitude ratio, phase shift, oscillation center shift, and control the noise level. Figure 4 shows some examples of the test signals.

The state of the two signals was controlled using the parameters shown in Table 1. Each parameter was

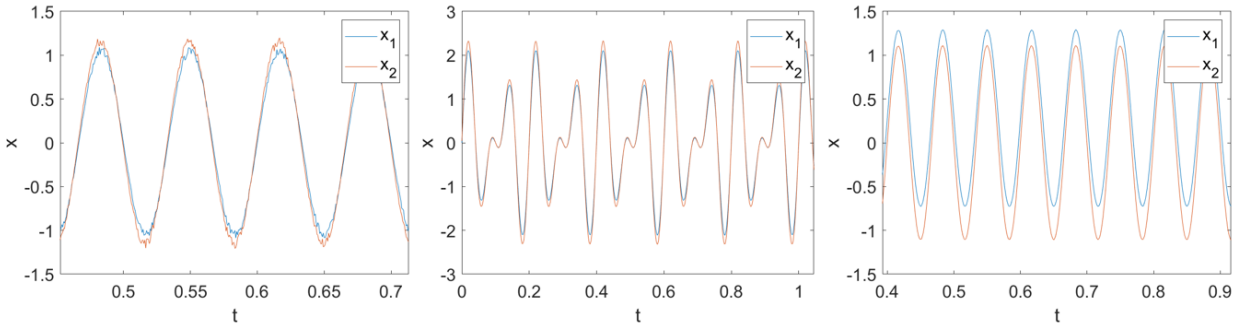

Figure 4: Examples of the signals used for testing the efficiency of Hilbert transformation and NLF methods.

varied within a given range to generate 1000 samples per test, assessing the ability of both the Hilbert and NLF methods to correctly estimate the forced phase shift and amplitude ratio.

Table 1 provides a clear comparison of relative estimation errors for each method. While the NLF method generally exhibits better accuracy when it comes to estimating the amplitude ratio, the Hilbert method still maintains a good overall performance as long as the the oscilation center of the signal does not shift by more that 20% of its amplitude. However, for the phase shift, the two methods seems to have the same level of accuracy with Hilbert being slightly superior. According to the nature of the experimental signals, the appropriate method will be utilized.

Table 1: The efficiency of Hilbert transformation and NLF in estimating the amplitude ratio and the phase shift for varying pairs of signals

	Range of the parameter value	Relative error estimating the Aplitude Ratio		Relative error estimating the Phase Shift	
		Hilbert	NLF	Hilbert	NLF
Referance Case	-	9.42E-06	1.17E-05	3.06E-03	8.06E-03
Amplitude ratio $\frac{x_2}{x_1}$	[0.7 ; 1.33]	1.02E-05	1.03E-05	2.95E-03	7.49E-03
phase shift $x_2 - x_1$ in degrees	[0.1 ; 0.19]	1.25E-05	1.38E-05	2.10E-02	5.29E-02
phase shift $x_2 - x_1$ in degrees	[2 ; 3]	4.03E-06	4.96E-06	1.31E-03	3.04E-03
uncentering ratio*	[0.01 ; 0.02]	9.64E-05	8.22E-06	2.88E-03	7.50E-03
uncentering ratio*	[0.2 ; 0.3]	1.50E-02	8.45E-06	8.87E-03	8.10E-03
noise ratio*	[0.1 ; 0.28]	1.03E-04	1.04E-04	2.81E-02	7.24E-02
Amplitude of the 2nd sine*	[1 ; 2.8]	2.71E-04	3.79E-05	1.38E-02	2.67E-02
Average relative error	-	1.94E-03	2.49E-05	1.03E-02	2.33E-02

*ratio of the signal's amplitude

3 Results

3.1 Data Collection

As explained in 2.2.1, a set of 14 tests were implemented and the FRF around the critical mode resulting from a random excitation is shown in Figure 5. After that, a manual sweep up and down the detected values was performed to accurately identify the mode for each different state of the structure. The experimental modes for the low excitation level were matching the ones we got directly from the random excitation tests, whereas they were shifted down by around 50 hz for the high excitation level case.

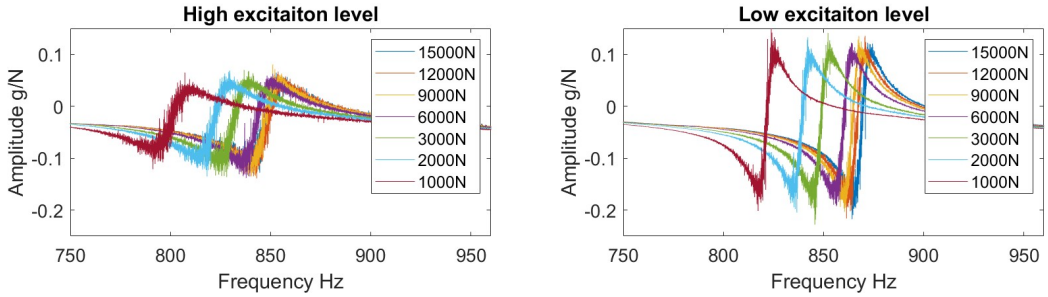

Figure 5: Excitation point FRF from a random excitation test for different tightening level and different excitation levels.

Despite the fact that the FRFs for the low excitation level case appear healthier, both cases show the same trend where the natural frequency drops with loosening. It is also worth noting that the frequency drop becomes more pronounced when the tightening level at the fan-hub interface becomes lower than 9000 N. The natural frequency defined for each case is presented in Table 2.

After each mode identification process, the structure was subjected to a pure sine signal with the same frequency. Throughout this test, the tightening level of the bolts was monitored for any potential changes, ultimately showing consistent values from the beginning to the end of the test, with minimal noise ranging from ± 0.5 N to ± 5 N between the highest and lowest tightening levels. Furthermore, data were collected from the two accelerometers mounted on each side of the interface, which is analyzed in detail in the following section. This analysis focused primarily on the response in the X direction, the primary direction of vibration in the targeted mode. See Figure 6.

Table 2: The critical torsion mode frequency for different states of the structure as defined experimentally.

Tightening Level N	High excitation level mode Hz	low excitation level mode Hz
15000	797	869
12000	797	867
9000	796	865
6000	792	861
3000	781	849
2000	772	840
1000	753	822

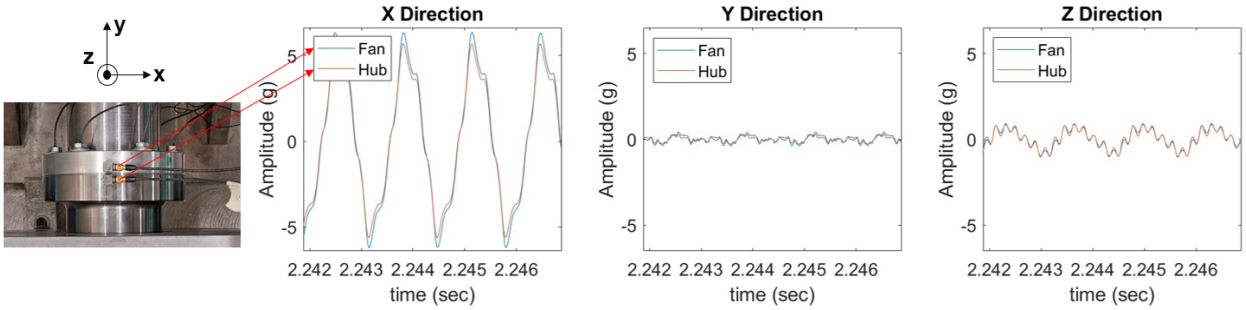

Figure 6: Time response at the fan-hub interface undergoing high excitation with bolts tightened to 1000 N.

3.2 Post processing

3.2.1 Intra-side signal comparison

Considering the structural status at 15000 N tightening level as a reference state, the cross-correlation and the P-value for t-test results are shown in Figure 7.

From the cross-correlation results, we observe a significant decrease in value immediately following the 12000 N case, indicating a possible drastic change in the signal when losing more than 3000 N of tightening force. This observation did not hold for all the conducted set of test at the low excitaion level, for instance, the set presented in Figure 7 shows a more gradual deterioration. However, the order of magnitude becomes the same across all the conducted tests and for both excitation levels after 6000 N. On the other hand, the P-value did not show any consistent trend when varying the tightening level, moreover, it was above the threshold for rejecting the null hypothesis for all structural states, indicating no significant shift in the oscillation center.

3.2.2 Inter-side signal comparison

Having studied the time response evolution for each side of the interface independently, we can now analyze the differences between the responses on both sides in terms of amplitude, phase, and the rate of change of these differences as the bolts loosen. As explained in Section 2.2.2, both the NLF and Hilbert transformation methods have their respective advantages and disadvantages for detecting the amplitude ratio and phase shift between two given signals. However, as shown in Section 3.2.1, the oscillation center has a negligible shift. Therefore, both methods exhibit the same level of accuracy for detecting the amplitude ratio, while the Hilbert transformation remains slightly more accurate for the phase shift. Based on this, we can use the Hilbert transformation to detect both the amplitude ratio and phase shift with an estimated error of less than 0.01% for the amplitude ratio and 1% for the phase shift. The results are presented in Figure 8.

The first observation is that the amplitude on the fan side is slightly larger than that on the hub side, which is consistent with the FEM analysis. Additionally, it is clear that loosening has a minimal effect on the amplitude ratio between the two sides of the studied interface. Even with an excitation level 14 times higher, the difference is only noticeable at the lowest tightening level which is 1000 N. This indicates that loosening

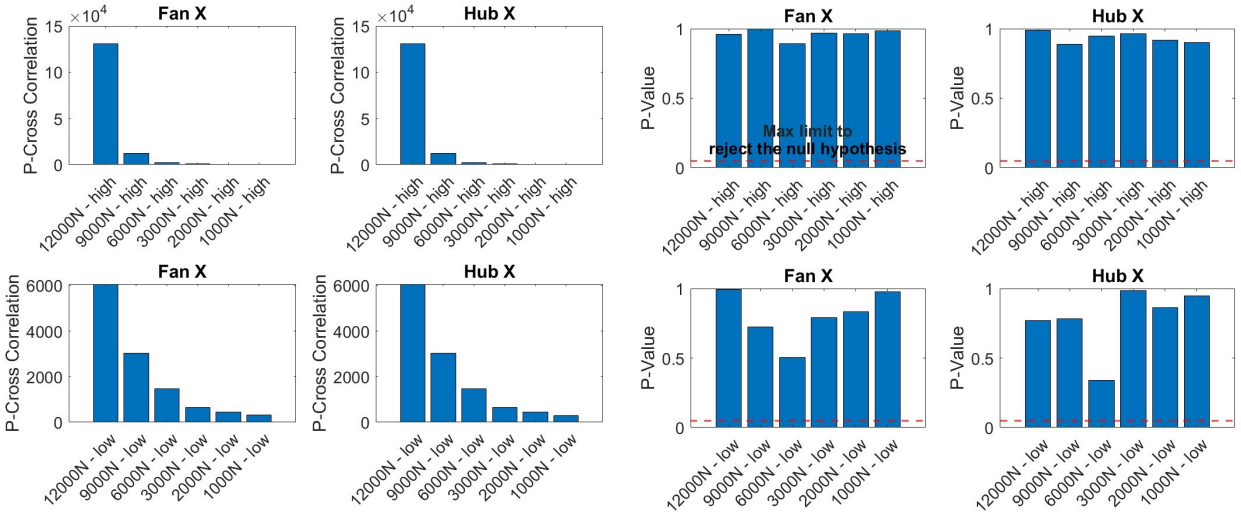

(a) Cross-correlation - max value (b) P-Value of t-test

Figure 7: Intra-side signal comparison with the tightening level of 15000 N as the reference case for both high and low excitation levels.

Figure 8: The evolution of the amplitude ratio and the phase shift between the fan side and the hub side with different tightening levels.

at the fan joint is unlikely to cause breakage in the fan body, as the tightening would need to drop more than 93% of its nominal value for the vibration amplitude to increase by 10%. On the other hand, the impact of bolt loosening on the phase between the two sides is more pronounced. Higher excitation levels result in bigger phase shifts, moreover, the rate at which the phase shift changes becomes higher with higher excitation levels and lower tightening levels.

Although the phase shift seems to decrease when going towards lower tightening levels, in extreme cases, as demonstrated by one case in Figure 8, it can increase drastically. This increase can potentially lead to fretting and subsequently to fretting fatigue at the interface, bearing in mind that the high excitation levels applied in our experimental tests (with a measured average of about 170 N) are approximately half what is needed to match the operational levels.

4 Conclusion

This study addressed the detection of bolt loosening as well as its impact on the mechanical integrity of the electric motor's fan. A set of 14 structured tests were conducted three times to ensure repeatability. The conventional mode shift indicator was employed to observe the impact of the bolts loosening on the

vibration behavior, alongside time response analysis. As a first step, the time response on each side of the fan-hub interface was analyzed independently, observing how it varies when the bolts are loosened. After that the signals were compared at the same tightening level in terms of amplitude and phase shift, analyzing how these difference will evolve with the systematic decrease of the tightening levels. The Hilbert transformation was utilized to achieve this purpose after thorough testing for compatibility and accuracy on synthetic user controlled signals. Results showed that while loosening is unlikely to cause a breakage in the fan due to an amplified response, the phase shift may increase significantly with high excitation and lower tightening levels, which could potentially lead to fretting at the interface. The suggested approach successfully provided a clear understanding of the relationship between the fan's vibration behavior and the health of its bolted joint. This understanding could be further enhanced by improving the experimental setup to apply higher excitation levels which better matches operational conditions, in addition to studying the long-term impact through extended duration vibration tests.

References

[1] Y. Lu, P. Xiang, P.-s. Dong, X. Zhang, and J. Zeng, "Analysis of the effects of vibration modes on fatigue damage in high-speed train bogie frames," *Engineering Failure Analysis*, vol. 89, pp. 222–241, 2018.

[2] L. Mao, W. Wang, Z. Liu, G. Yang, C. Song, and S. Qu, "Research on causes of fatigue cracking in the motor hangers of high-speed trains induced by current fluctuation," *Engineering Failure Analysis*, vol. 127, p. 105508, 2021.

[3] W. Hu, Z. Liu, D. Liu, and X. Hai, "Fatigue failure analysis of high speed train gearbox housings," *Engineering Failure Analysis*, vol. 73, pp. 57–71, 2017.

[4] Y. Hu, J. Lin, and A. C. Tan, "Failure analysis of gearbox in crh high-speed train," *Engineering Failure Analysis*, vol. 105, pp. 110–126, 2019.

[5] Y. Hu, A. C. Tan, C. Liang, and Y. Li, "Failure analysis of fractured motor bolts in high-speed train due to cardan shaft misalignment," *Engineering Failure Analysis*, vol. 122, p. 105246, 2021.

[6] F. P. Sun, Z. Chaudhry, C. Liang, and C. Rogers, "Truss structure integrity identification using pzt sensor-actuator," *Journal of Intelligent material systems and structures*, vol. 6, no. 1, pp. 134–139, 1995.

[7] M. Derriso, W. Braisted, J. Rosenstengel, and M. DeSimio, "The structural health monitoring of a mechanically attached thermal protection system," *JOM*, vol. 56, no. 3, pp. 36–39, 2004.

[8] D. M. Peairs, G. Park, and D. J. Inman, "Practical issues of activating self-repairing bolted joints," *Smart Materials and Structures*, vol. 13, no. 6, p. 1414, 2004.

[9] J. Yang and F.-K. Chang, "Detection of bolt lngoosening in c–c composite thermal protection panels: I. diagnostic principle," *Smart Materials and Structures*, vol. 15, no. 2, p. 581, 2006.

[10] J. Yang and F.-K. Chang, "Detection of bolt loosening in c–c composite thermal protection panels: Ii. experimental verification," *Smart Materials and Structures*, vol. 15, no. 2, p. 591, 2006.

[11] S. Chaki and G. Bourse, "Stress level measurement in prestressed steel strands using acoustoelastic effect," *Experimental Mechanics*, vol. 49, pp. 673–681, 2009.

[12] Q. Sun, B. Yuan, X. Mu, and W. Sun, "Bolt preload measurement based on the acoustoelastic effect using smart piezoelectric bolt," *Smart Materials and Structures*, vol. 28, no. 5, p. 055005, 2019.